

Comparative study of different methods of preparing CuO-CeO₂ catalysts for preferential oxidation of CO in excess hydrogen

Zhigang Liu, Renxian Zhou*, Xiaoming Zheng

Institute of catalysis, Zhejiang University, Hangzhou 310028, PR China

Received 26 May 2006; received in revised form 11 November 2006; accepted 19 November 2006

Available online 25 November 2006

Abstract

Influence of preparation methods (i.e. co-precipitation, chelating, citric acid and critical phase) on the preferential oxidation of CO in excess hydrogen over CuO-CeO₂ catalysts has been investigated. CuO-CeO₂ catalysts are characterized by using BET, X-ray powder diffraction (XRD), UV Raman and temperature-programmed reduction (TPR) techniques. The catalyst prepared by chelating is most active for the preferential oxidation of CO. In addition, XRD, UV Raman and TPR show that the chelating method enhances the formation of defects of ceria and produces a synergic effect between the cycle of Cu¹⁺/Cu²⁺ and that of Ce³⁺/Ce⁴⁺, which is beneficial to the improvement of the performance of CuO-CeO₂ catalysts. © 2006 Elsevier B.V. All rights reserved.

Keywords: CuO-CeO₂; Preferential oxidation; CO; Fuel cell; Preparation method

1. Introduction

Recently, the CuO-CeO₂ catalyst has been attracting attentions because of its activity higher than that of conventional copper-based catalysts and comparable or superior to that of platinum catalysts for the preferential oxidation of CO in excess hydrogen [1–5], which has been used for PEM fuel cells (PEM-FCS). It is believed that the reaction is catalyzed by the interfacial copper oxide-ceria centers in which ceria presents a high number of oxygen vacancies that permits a high mobility of lattice oxygen [6,7].

For CuO-CeO₂ catalysts, preparation methods have a critical influence on preferential oxidation of CO in excess hydrogen. Preparation methods reported are co-precipitation [8–10], urea-nitrate combustion method [11,12], sol-gel peroxo route [13,14], etc. Avgouropoulos et al. [15] investigated the difference among four CuO-CeO₂ catalysts prepared by using the co-precipitation, the citrate-hydrothermal, the urea-nitrates combustion and the impregnation methods. They found that the combustion-prepared sample exhibited the best catalytic performance, followed by the citrate-hydrothermally-prepared sample. The impregnated one was least active. However,

CuO-CeO₂ catalysts synthesized by Kim and Cha [3] using co-precipitation methods, with a BET specific surface area of 91 m²/g, showed superior performance in the preferential oxidation of CO in excess hydrogen; i.e., these catalysts reduced the CO content to less than 100 ppm at the temperature below 170 °C for a feed of 1% CO, 1% or 1.25% O₂, 50% H₂ in the presence of H₂O and CO₂. Obviously, the preparation methods had a marked effect on the performance of CuO-CeO₂ catalysts in the preferential oxidation of CO.

In this work, influence of the preparation methods (i.e. co-precipitation, chelating, citric acid and critical phase) on the preferential oxidation of CO in excess hydrogen over CuO-CeO₂ catalysts has been investigated, and the catalysts have been characterized by BET, X-ray powder diffraction (XRD), UV Raman and temperature-programmed reduction (TPR) techniques. The catalyst prepared by chelating gave a catalytic performance in the preferential oxidation of CO superior to the catalysts prepared by the other preparation methods.

2. Experimental

2.1. Catalyst preparation

Sample 1 (designated as 5CuC-CP) was synthesized by co-precipitation from the mixture (250 ml) of 0.055 mol/l Ce(NO₃)₂

* Corresponding author. Tel.: +86 571 88273272; fax: +86 571 88273283.
E-mail address: zhourenxian@zju.edu.cn (R. Zhou).

and 0.008 mol/l $\text{Cu}(\text{NO}_3)_2$. 0.362 mol/l KOH was added dropwise with vigorous stirring, and then the mixture was aged for about 20 min. The pH value of the mixture was 12.5 and the obtained precipitate was washed with distilled water until pH was decreased to 7.0, followed by washing with 200 ml ethanol before being dried at 105 °C for about 3 h. The dried sample was thermally treated at 500 °C for about 2 h.

Sample 2 (designated as 5CuC-CE) was synthesized by drying under a critical phase of ethanol. The other steps were similar to those for the co-precipitation-prepared sample.

Sample 3 (designated as 5CuC-CH) was synthesized by the chelating method. The solution of cetyltrimethylammonium bromide ($\text{C}_{19}\text{H}_{42}\text{BrN}$) was added dropwise into the mixture of 0.055 mol/l $\text{Ce}(\text{NO}_3)_2$ and 0.008 mol/l $\text{Cu}(\text{NO}_3)_2$ solutions with vigorous stirring, and the obtained sol–gel was aged for 30 min at ambient temperatures. It should be noted that all the solvent in the experiment is not water but ethanol. Then, the sol–gel was dried at 100 °C for about 5 h and then thermally treated at 500 °C for 2 h.

Sample 4 (designated as 5CuC-CA) was prepared by the citric acid method. Aqueous solution of 0.060 mol/l citric acid was added dropwise into the mixture of equal amount of 0.055 mol/l $\text{Ce}(\text{NO}_3)_2$ and 0.008 mol/l $\text{Cu}(\text{NO}_3)_2$ under continuous stirring and then the mixture was kept stirring for 6 h. The mixed solution was dried at 120 °C for a few hours to obtain the powder, followed by thermal treatment at 500 °C for 2 h.

All treated catalysts were crushed and sieved to 60–80 meshes. The Cu content over all the catalysts was expressed as the $\text{Cu}/(\text{Cu} + \text{CeO}_2)$ wt% ratio and all data below were obtained with 5.0 wt% Cu catalysts.

2.2. Measurement of catalytic performance

The activity measurement was carried out in a fixed-bed micro-reactor (quartz glass, i.d. 4 mm, o.d. 6 mm, length 250 mm) at atmospheric pressure. The reactor temperature was measured with a K-type thermocouple located at the top of the packed catalyst bed and controlled by a temperature controller. The mass of catalyst used in the experiments was 50 mg, and the

catalyst was diluted with inert alumina particles (60–80 meshes) with a mass ratio of 1:1. A desired mixture of gases (i.e. 50% H_2 , 1.0% O_2 , 1.0% CO and Ar in balance) was prepared by adjusting the ratio of flows with the mass flow controllers (Scientific Alicat). The steam was introduced with reacting gases bubbling through a thermostat water bath.

The reactor inlet and outlet streams were measured using an on-line gas chromatograph equipped with a thermal conductivity detector (TCD) and a flame ionization detector (FID). H_2 and O_2 were separated by a carbon molecular sieve (TDX-01) column and detected with TCD. CO and CO_2 were separated by a carbon molecular sieve (TDX-01) column, then converted to methane by a methanation reactor and analyzed by FID. The detection limit of FID for CO is less than 3 ppm.

Taking into consideration of the existence of CO_2 in the feedstock, the CO conversion was calculated based on the CO decrease as follows:

$$\% \text{ of conversion of CO} = \frac{[\text{CO}]_{\text{in}} - [\text{CO}]_{\text{out}}}{[\text{CO}]_{\text{in}}} \times 100$$

The selectivity was defined as the oxygen consumed by CO oxidation, namely:

$$\% \text{ of selectivity} = \frac{0.5([\text{CO}]_{\text{in}} - [\text{CO}]_{\text{out}})}{[\text{O}_2]_{\text{in}} - [\text{O}_2]_{\text{out}}} \times 100$$

2.3. Characterization of catalysts

The specific area of the sample was obtained at -196 °C using a Coulter Omnisorp 100CX. Prior to the measurement, the sample was pretreated at 250 °C for 2 h. X-ray powder diffraction patterns were recorded on a Rigaku D/Max 2550PC powder diffractometer using nickel-filtered $\text{Cu K}\alpha$ radiation. UV Raman spectra were recorded on a UV-HR Raman spectrograph. The laser power measured at the samples was below 4.0 mW for 325 nm radiation. H_2 temperature-programmed reduction was carried out using a conventional reactor equipped with TCD. Fifty milligrams catalyst and 40 ml/min flowing velocity of 5% H_2/Ar were applied in this work. The temperature rate was 10 °C/min from 30 °C to 570 °C.

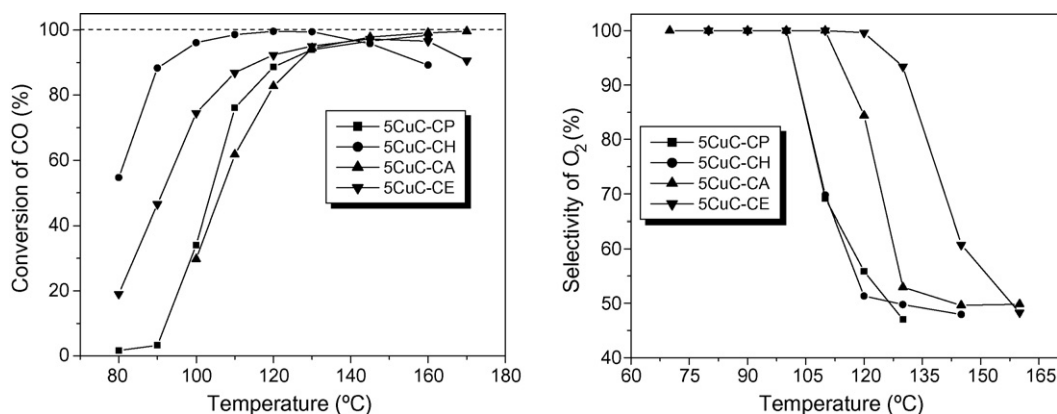


Fig. 1. The activity and selectivity of CuO-CeO_2 catalysts prepared with different preparation methods, at a space velocity of $120,000 \text{ ml g}^{-1} \text{ h}^{-1}$, in a feed of 1.0% CO, 1.0% O_2 , 50% H_2 , balance Ar.

3. Results and discussion

3.1. The catalytic performance of CuO-CeO₂ catalysts

The preferential oxidation of CO in excess hydrogen over the CuO-CeO₂ catalysts prepared by different methods is illustrated in Fig. 1. From Fig. 1, it can be seen that the preparation methods have a significant influence on the catalytic performance of CuO-CeO₂ catalysts. 5CuC-CH exhibits the highest catalytic activity in the preferential oxidation of CO and 5CuC-CA shows the lowest catalytic activity. T_{60} (i.e. the temperature required for 60% conversion of CO) for 5CuC-CP, 5CuC-CH, 5CuC-CA and 5CuC-CE are 106 °C, 81 °C, 109 °C and 95 °C, respectively. However, in the temperature range from 60 °C to 160 °C, the highest conversions of CO appear in the light-off curves of the catalysts, and the corresponding temperatures for 5CuC-CP, 5CuC-CH, 5CuC-CA and 5CuC-CE are 160 °C (98.0% of CO conversion), 120 °C (99.6% of CO conversion), 160 °C (99.2% of CO conversion) and 145 °C (97.3% of CO conversion), respectively. In addition, at a space velocity of 120,000 ml g⁻¹ h⁻¹, 5CuC-CP and 5CuC-CE cannot reach CO conversion higher than 99.0% (namely the CO concentration less than 100 ppm) in contrast with 5CuC-CH and 5CuC-CA attaining CO conversion higher than 99.0%. It is evident that 5CuC-CH shows outstanding catalytic activity in the preferential oxidation of CO in excess hydrogen compared with 5CuC-CP, 5CuC-CA and 5CuC-CE.

The selectivity of O₂ shows a contrary trend with the increase in reaction temperatures, due to the fact that displacement of adsorbed hydrogen by carbon monoxide and blocking of hydrogen adsorption by preadsorbed carbon monoxide occur during the competing adsorption of hydrogen and carbon monoxide [16]. For example, in case of 5CuC-CH, the selectivity declines from 100.0% at 100 °C to about 48.0% at 145 °C. In addition, for 5CuC-CA and 5CuC-CE, 100% selectivity of O₂ is still observed at 110 °C. Consequently, 5CuC-CH has a lower selectivity of O₂ than 5CuC-CA and 5CuC-CE.

Fig. 2 illustrates the influence of the space velocity. As seen from Fig. 2, increase in the space velocity has a negative effect on the performance of CuO-CeO₂ catalysts prepared with the chelating method. At the space velocity of 120,000 ml g⁻¹ h⁻¹, the CO conversion and selectivity of O₂ over CuO-CeO₂ catalyst are slightly lower than at 30,000 ml g⁻¹ h⁻¹.

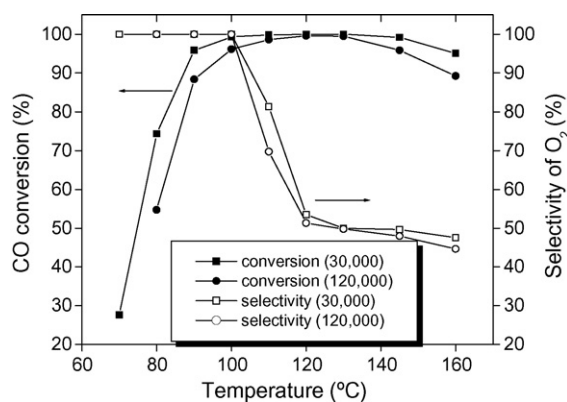


Fig. 2. The influence of the space velocity on the catalytic performance of CuO-CeO₂ catalyst prepared with the chelating method, at a space velocity of 30,000–120,000 ml g⁻¹ h⁻¹, in a feed of 1.0% CO, 1.0% O₂, 50% H₂, balance Ar.

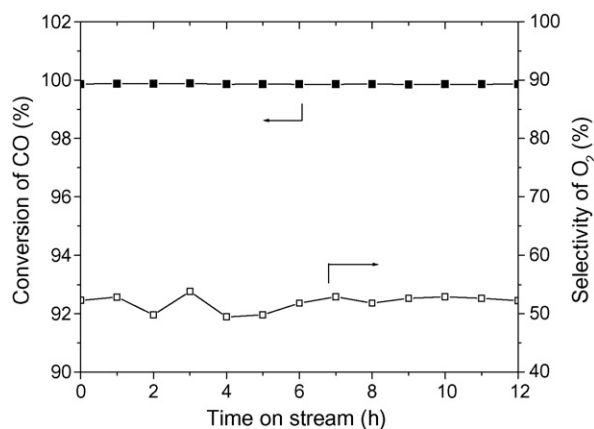


Fig. 3. Time on stream over the CuO-CeO₂ catalyst prepared with the chelating method at 120 °C.

In order to investigate the stability of 5CuC-CH and eliminate the influence of initial activity of CuO-CeO₂ catalysts on the measurement of activity, the duration test is run for 12 h at 120 °C and 120,000 ml g⁻¹ h⁻¹ of GHSV in a feed of 1% CO, 1% O₂, 50% H₂ and Ar in balance. As shown in Fig. 3, the CO conversions is kept at the values higher than 99% during the run. Selectivity of O₂ exhibits a slight increase, about 1% in the end of the test. It is evident that 5CuC-CH possesses a desirable stability, which is consistent with some literature [2,3]. Thus,

Table 1
Characteristics of CuO-CeO₂ catalysts and comparison of their activity in CO oxidation

Catalysts	S_{BET} (m ² /g)	PV (ml/g) ^a	APD (nm) ^b	r_{CO} at 100 °C ^c			T_{60} (°C) ^d
				$\mu\text{mol}_{\text{CO}}$ (s g _{cat}) ⁻¹	$\mu\text{mol}_{\text{CO}}$ (s g _{Cu}) ⁻¹	$\mu\text{mol}_{\text{CO}}$ (s m ²) ⁻¹	
5CuC-CP	111	0.22	7.9	5.2	104	0.047	106
5CuC-CH	99	0.18	7.3	14.4	288	0.145	81
5CuC-CA	31	0.16	20.6	4.4	88	1.419	109
5CuC-CE	89	0.16	7.2	11.2	224	0.126	95

^a PV, pore volume.

^b APD, average pore diameter (APD = 4 × pore volume/BET surface area).

^c According to literature [7].

^d $W/F = 0.03 \text{ g s cm}^{-3}$.

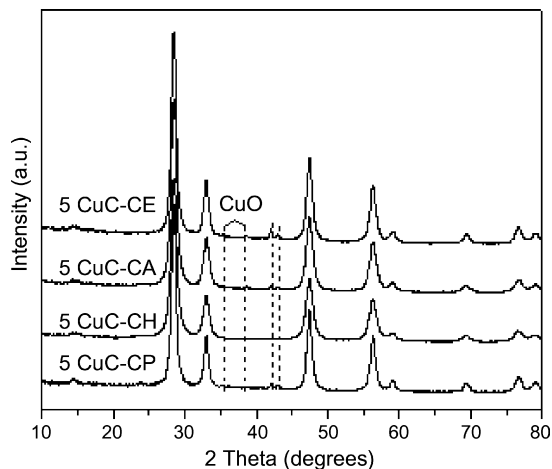


Fig. 4. XRD patterns of CuO-CeO₂ catalysts prepared by different methods.

the influence of initial activity of CuO-CeO₂ catalysts on the measurement of activity is eliminated.

3.2. The structural studies of CuO-CeO₂ catalysts

Table 1 lists the pore volume, average pore diameter and surface areas and catalytic activity of the CuO-CeO₂ catalysts prepared by different methods. From Table 1, it can be seen that 5CuC-CP has the largest BET area (111 m² g⁻¹) and the lowest TOF (0.047 μmol_{CO} (s m²)⁻¹), while 5CuC-CA has a BET area of only about one third of that of 5CuC-CP and the highest TOF (1.419 μmol_{CO} (s m²)⁻¹). 5CuC-CH with a surface area of 99 m² g⁻¹ achieves the highest activity in preferential oxidation of CO. Namely T₆₀ of 5CuC-CH is as low as 81 °C, compared with 109 °C over 5CuC-CA and 106 °C over 5CuC-CP.

Fig. 4 shows the XRD patterns of CuO-CeO₂ catalysts prepared by different preparation methods. It can be seen that the distinct fluorite-type oxide structure of CeO₂ is observed in all samples [17], and that the peaks of 5CuC-CH are broader than those of other catalysts, which indicates that 5CuC-CH has a smaller particle size than the other catalysts. In addition, four peaks can be found at 36°, 38.6°, 42° and 43°. Peaks at 36° and 38.6° are assigned to the peak of crystal CuO. The peaks of CuO appear in the XRD patterns of 5CuC-CP, 5CuC-CA and 5CuC-CE. However, no peaks of CuO can be seen in that of 5CuC-CH, which means that CuO is well dispersed in 5CuC-CH. Two peaks at 42° and 43° are assigned to the formation of cerium and copper solid solution. The peaks of cerium and copper solid solution appear in the XRD patterns of 5CuC-CP, 5CuC-CA and 5CuC-CE. No peaks of cerium and copper solid solution can be seen in that of 5CuC-CH. However, it should also be noted that the XRD peaks of CeO₂ are rather broad and shifts of small magnitude cannot be detectable. Therefore, the possibility of existence of trace copper and cerium solid solution cannot be excluded.

Fig. 5 shows the UV Raman spectra recorded by using a laser at 325 nm as the excitation source. A broad band with relatively high intensity at 462 cm⁻¹ is assigned to cubic CeO₂ in CuO-CeO₂ catalysts together with two bands at 584 cm⁻¹ and 1176 cm⁻¹ [12]. The bands at about 584 cm⁻¹ and 1176 cm⁻¹

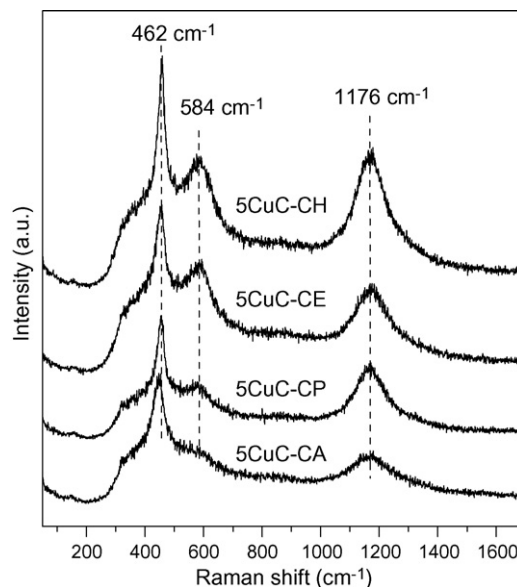


Fig. 5. UV Raman spectra of CuO-CeO₂ catalysts prepared by different methods.

can be linked to oxygen vacancies in the CeO₂ lattice and attributed to the CeO₂ defects [18,19]. It can also be seen that the intensity of 584 cm⁻¹ and 1176 cm⁻¹ bands of CuO-CeO₂ catalysts builds up with the increase in the turn of 5CuC-CP, 5CuC-CE, 5CuC-CA and 5CuC-CH, which indicates that the amount of defects in CuO-CeO₂ catalysts is increased. Defects have a beneficial influence on the catalytic performance of CuO-based catalysts in preferential oxidation of CO in excess hydrogen [20]. Consequently, the amount of defects correlates well with the activity of CuO-CeO₂ catalysts.

The H₂-TPR profiles of CuO-CeO₂ catalysts prepared by different methods are illustrated in Fig. 6. From Fig. 6, it can be seen that the overlapping reduction peaks of CuO_x species, for 5CuC-CP, 5CuC-CE and 5CuC-CA, consist of a low-intensity, low-temperature peak at about 161 °C (α peak) and a higher-

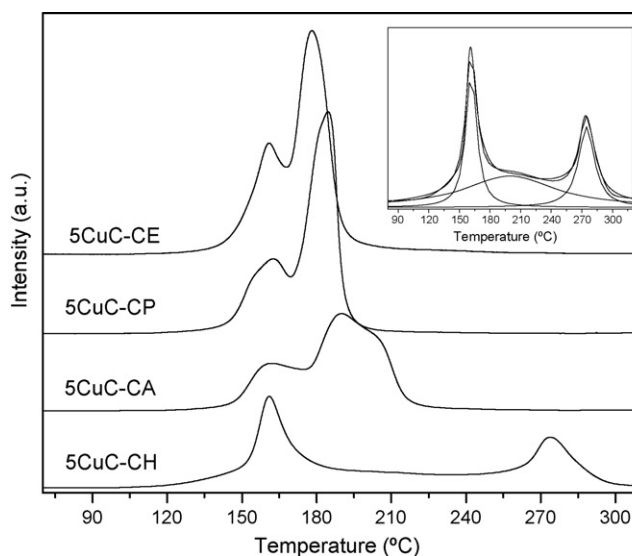


Fig. 6. TPR profiles of CuO-CeO₂ catalysts prepared by different methods.

Table 2
H₂ consumption and temperature of TPR peaks for catalysts prepared by different methods

Catalysts	α peak		β peak		β' or γ peak	
	H ₂ consumption ($\mu\text{mol/g}_{\text{cat}}$)	Peak temperature ($^{\circ}\text{C}$)	H ₂ consumption ($\mu\text{mol/g}_{\text{cat}}$)	Peak temperature ($^{\circ}\text{C}$)	H ₂ consumption ($\mu\text{mol/g}_{\text{cat}}$)	Peak temperature ($^{\circ}\text{C}$)
5CuC-CP	325	162.6	479	183.1		
5CuC-CH	295	161.7	568	199.5	256	274.6
5CuC-CA	199	161.8	522	189.8	157	203.7
5CuC-CE	312	160.5	551	178.9		

intensity peak at about 180 $^{\circ}\text{C}$ (β peak). In addition, a shoulder peak is found at 203.7 $^{\circ}\text{C}$ in the case of 5CuC-CA, and assigned to β' peak. Generally, there are several types of copper-oxygen entities [20,21]: (a) isolated Cu^{2+} ions can strongly interact with the support; (b) weak magnetic associates consist of several Cu^{2+} ions and these Cu^{2+} ions have close contact with each other; (c) small two- and three-dimensional clusters have so loose structures that they have no specific and regular lattice arrangement; (d) large three-dimensional clusters and bulk CuO phase have characters and properties identical to those of pure CuO powder. Therefore, in this work, α peak may be attributed to a type or b type, β peak may be assigned to c type and γ or β' peak may be assigned to d type.

However, for 5CuC-CH, not only α peak at 161.7 $^{\circ}\text{C}$ but also γ peak at 274.6 $^{\circ}\text{C}$ is found. There is an overlapping reduction peak between α peak and γ peak. H₂ consumptions of α , β and γ peaks are (multi-peaks fitted according to the Lorentz method and shown in Table 2) 295 $\mu\text{mol/g}_{\text{cat}}$, 568 $\mu\text{mol/g}_{\text{cat}}$ and 256 $\mu\text{mol/g}_{\text{cat}}$, respectively. The amount of H₂ consumption for α , β and γ peaks are 1119 $\mu\text{mol/g}_{\text{cat}}$ and larger than the theoretical amount of H₂ consumption in 5CuC-CH (i.e. 787 $\mu\text{mol/g}_{\text{cat}}$). Furthermore, in Fig. 7, CeO₂-CH (prepared by the chelating method) has two peaks in the TPR profile, one at 414 $^{\circ}\text{C}$ and the other at 513 $^{\circ}\text{C}$. When copper oxide and cerium oxide is prepared by the chelating method, 5CuC-CH exhibits H₂ reduction peaks well below 450 $^{\circ}\text{C}$. Obviously, the reduction of surface or bulk oxygen species of ceria is involved, which indicates that ceria has an amount of copper oxide dissolved in it. The amount of copper oxide, even though perhaps small, is large

enough to change its oxide ion transport properties and enable bulk reduction at 400 $^{\circ}\text{C}$ [9].

In addition, γ peaks in TPR patterns of 5CuC-CH cannot be assigned to the reduction of bulk CuO. If γ peak were assigned to the reduction of bulk CuO, signal of bulk CuO should have been strong enough to be seen in the XRD pattern, due to the existence of large amount of bulk CuO. However, in the case of 5CuC-CH, bulk CuO or solid solution of copper and cerium cannot be found in the XRD patterns, which indicates that some other species are reduced at the position of γ peak.

In general, pure CuO and Cu₂O catalysts exhibit H₂ reduction peaks at approximately 180 $^{\circ}\text{C}$ and 300 $^{\circ}\text{C}$ [22]. Therefore, α and γ peaks may be assigned to the reduction of CuO and Cu₂O, respectively. Moreover, Fig. 8 indicates the influence of redox cycles on reducibility of 5CuC-CH. With the increase in redox cycles, α peak shifts to higher temperature and β peaks appear between α and γ peaks, while the position of γ peaks slightly changes. Thus, β peak is assigned to the reduction of CuO with larger particle sizes.

According to above discussion, the reduction of 5CuC-CH includes several types: (a) reduction of CuO with small particle sizes; (b) reduction of CuO with large particle sizes; (c) reduction of Cu₂O; (d) reduction of surface or bulk oxygen species of ceria. During the reduction of 5CuC-CH the equilibrium of the above reduction types can be expressed as follow [23,24]:



This equilibrium can stabilize the cationic copper species in the structure even in highly reductive atmosphere [9]. If so, the high

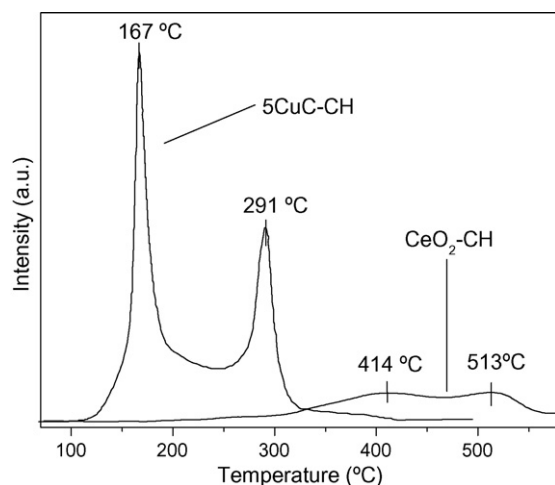


Fig. 7. TPR profiles of 5CuC-CH and CeO₂-CH.

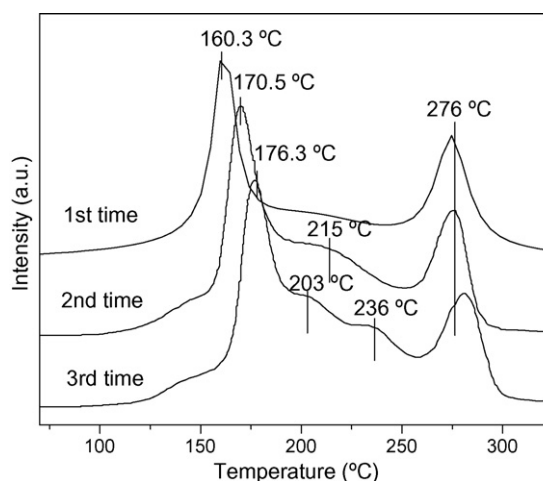


Fig. 8. TPR profiles of 5CuC-CH reoxidized with different times.

activity of CO oxidation in excess hydrogen over 5CuC-CH can evolve as a synergic effect between the cycle of $\text{Cu}^{1+}/\text{Cu}^{2+}$ and that of $\text{Ce}^{3+}/\text{Ce}^{4+}$.

4. Conclusions

In this work, the influence of preparation methods (i.e. co-precipitation, chelating, citric acid and critical phase) on the preferential oxidation of CO in excess hydrogen over CuO-CeO₂ catalysts has been investigated and CuO-CeO₂ catalysts are characterized by using BET, XRD, UV Raman and TPR techniques. The catalyst prepared by chelating is most active in preferential oxidation of CO. CO conversion over 5CuC-CH is 99.6% at the temperature of 120 °C, while CO conversions over 5CuC-CE and 5CuC-CP cannot reach 99% in all reaction temperature range and that over 5CuC-CA is 99.2% at the temperature of 160 °C. In addition, the chelating method enhances the formation of defects of ceria and produces a synergic effect between the cycle of $\text{Cu}^{1+}/\text{Cu}^{2+}$ and that of $\text{Ce}^{3+}/\text{Ce}^{4+}$, which are beneficial to the improvement of the performance of CuO-CeO₂ catalysts.

Acknowledgment

The authors gratefully acknowledge the Ministry of Science and Technology of China (No: 2004 CB 719504).

References

- [1] W. Liu, M. Flytzani-Stephanopoulos, Chem. Eng. J. 64 (1996) 283.
- [2] G. Avgouropoulos, T. Ioannides, H.K. Matralis, Catal. Lett. 73 (2001) 33.

- [3] D.H. Kim, J.E. Cha, Catal. Lett. 86 (2003) 107.
- [4] P. Chin, X.L. Sun, G.W. Roberts, J.J. Spivey, Appl. Catal. A: Gen. 302 (2006) 22.
- [5] K. Tanaka, Y. Moro-oka, K. Ishigure, et al., Catal. Lett. 92 (2004) 115.
- [6] J.B. Wang, W.H. Shih, T.J. Huang, Appl. Catal. A: Gen. 203 (2000) 191.
- [7] W. Liu, M. Flytzani-Stephanopoulos, J. Catal. 153 (1995) 304.
- [8] G. Avgouropoulos, T. Ioannides, Appl. Catal. A 244 (2003) 155.
- [9] G. Sedmak, S. Hocevar, J. Levec, J. Catal. 213 (2003) 135.
- [10] D.H. Kim, M.S. Lim, Appl. Catal. A 224 (2002) 27.
- [11] G. Avgouropoulos, Th. Ioannides, Appl. Catal. A: Gen. 244 (2003) 155.
- [12] W. Shan, Z. Feng, Z. Li, J. Zhang, W. Shen, C. Li, J. Catal. 228 (2004) 206.
- [13] G. Avgouropoulos, T. Ioannides, Ch. Papadopoulou, J. Batista, S. Hocevar, H.K. Matralis, Catal. Today 75 (2002) 157.
- [14] Y. Liu, Q. Fu, M. Flytzani-Stephanopoulos, Catal. Today 93–95 (2000) 241.
- [15] G. Avgouropoulos, T. Ioannides, H.K. Matralis, Appl. Catal. B: Environ. 56 (2005) 87.
- [16] B.E. Nieuwenhuys, Surf. Sci. 126 (1983) 307.
- [17] V. Oerichon, A. Laachir, S. Abouarnadasse, O. Touret, G. Blanchard, Appl. Catal. A: Gen. 129 (1995) 69.
- [18] J.E. Spanier, R.D. Robinson, F. Zhang, S.W. Chan, I.P. Herman, Phys. Rev. B 64 (2001) 245407.
- [19] J.R. McBride, K.C. Hass, B.D. Poindexter, W.H. Weber, J. Appl. Phys. 76 (1994) 2435.
- [20] W.P. Dow, Y.P. Wang, T.J. Huang, J. Catal. 160 (1996) 171.
- [21] W.P. Dow, Y.P. Wang, T.J. Huang, J. Catal. 160 (1996) 155.
- [22] G. Fierro, M. Lo Jacono, M. Inversi, P. Porta, R. Lavecchia, F. Cioci, J. Catal. 148 (1994) 709.
- [23] S. Hocevar, J. Batista, J. Levec, J. Catal. 184 (1999) 39.
- [24] C. Lamonier, A. Ponchel, A. D'Huysser, L. Jalowiecki-Duhamel, Catal. Today 50 (1999) 247.